Osman *et al.*
Journal of Engineering and Applied Science (2023) 70:38
https://doi.org/10.1186/s44147-023-00210-y

Journal of Engineering and Applied Science

RESEARCH Open Access

Performance of externally reinforced CHS X-joints subjected to axial loads

Ashraf Osman[1*], Peter Gerguis[1] and Sameh Gaawan[2]

*Correspondence:
aosman@eng.cu.edu.eg

[1] Structural Engineering Department, Cairo University, Giza, Egypt
[2] Faculty of Engineering Mataria branch, Structures Department, Helwan University, Cairo, Egypt

Abstract

Circular hollow sections (CHS) have evolved as the primary choice for the tubular lattice structures, due to their excellent mechanical properties and aesthetic appearance. However, enhancing the joints capacities in such structures poses as challenge to structural designer. Recent research addressed several external reinforcing schemes that can be utilized for strengthening CHS X-joints. Although each of these schemes was studied thoroughly, no collective study was conducted to compare between their efficiencies in enhancing CHS X-joints strengths and stiffnesses. This study focuses on evaluating the structural performance of these techniques relative to each other. The results showed that CHS X-joints strengthened using outer flanged pipe to confine brace-chord intersection achieved the highest strength and stiffness enhancement among the examined joints. Also, it proved that joints strengthened with single or double outer stiffeners yielded acceptable capacity enhancement with the advantages of easy fabrication and acceptable aesthetically appearance.

Keywords: Circular hollow steel (CHS), Comparative study, Finite element, Stiffeners, X-Joint, Strengthening

Introduction

Recently, utilization of circular hollow sections (CHS) for construction of tubular lattice structures have evolved as the primary choice for engineers. Their high strength to-weight ratio, superior static, and dynamic behavior, in addition, to easy maintenance in severe environment made them the first choice for structural designers [9, 10]. However, the main weakness associated with using CHS sections in tubular latticed structures is the limited strength of joints. These joints, either T or X shaped, when subjected to axial compressive forces, failure usually occurs at chord members because the resistance of their walls to transverse forces is too limited to sustain the transferred brace forces. Observed failure patterns are manifested as chord plastification, chord local buckling, or punching shear whereas failure of brace members does not commonly occur. Therefore, full utilization of tubular structure sections capacities and economical design require enhancing joints capacities.

In the past decade, many researchers proposed different schemes for strengthening those crucial joints to enhance their nominal capacities. These strengthening schemes can be categorized into two main groups, namely, internal, and external reinforcing

methods. The first group includes providing internal stiffening rings to chord members at joints locations [2, 8, 23], filling chord with concrete at joints [7,5] and increasing the chord thickness at joint locations [22]. Although these schemes were proved to be efficient in enhancing joints capacities, they complicate the fabrication process and are only applicable to new fabricated joints. The second group involves the use of external stiffeners [13, 25, 28], external stiffening rings [27, 28, 15], fiber reinforced polymer (FRP) composite strengthening [11, 12, 21], doubler or collar-plate reinforcement [16–20] or outer flanged pipe to confine brace-chord intersection [6, 14] These techniques in addition of being efficient in enhancing joints capacities, they, are appropriate for strengthening both the new and pre-fabricated joints, with easiness from fabrication perspective. However, reviewing the available literature showed that there is still a dearth in knowledge regarding the comparative efficiency of these schemes in case they are utilized for strengthening CHS joints. Most research works in this field focused on examining the sole behavior of retrofitted joints without comparing between these efficiencies of these different strengthening schemes.

This research work provides a comparative study to evaluate the structural efficiency of four of those external strengthening schemes widely used for reinforcing CHS X-joints. The considered strengthening schemes were (1) adding external stiffeners as shown in joint type a in Fig. 1; (2) adding single outer ring stiffener at brace-chord intersection as shown in joint type b in Fig. 1; (3) adding two outer ring stiffeners near brace-chord intersection as shown in joint type c in Fig. 1; and (4) adding outer flanged pipe to confine brace-chord intersection as shown in joint type d in Fig. 1. It is worth to mention here that limiting the study to evaluate the efficiency of those external reinforcing schemes is attributed mainly to their common use, ease of fabrication, and capability for strengthening both new and prefabricated joints.

Within this context, the study evaluated the gain in CHS X-joints strengths and stiffnesses due to the employment of each of these four schemes when subjected to axial compressive forces. Effects of different joints geometrical parameters such as brace diameter-to-chord diameter ratio ($\beta = d_b/d_o$) and chord diameter-to-double the chord thickness ratio ($2\gamma = d_o/t_o$) in relation to the provided dimensions of utilizes stiffeners on enhancing joints strengths and stiffnesses were examined.

Methodology

The evaluation methodology followed in this study, was initiated by developing finite element models (FEM) for several experimentally tested reinforced and unreinforced CHS X-joints and calibrating their behaviors against experimental responses to verify the models' accuracies. Then, the same modelling approach was adopted to develop several numerical models for unreinforced joints with different geometrical parameters. Each of these joints was later strengthened using the previously described strengthening schemes and analyzed under the application of axial compressive forces. The gain in the strengths and stiffnesses of reinforced joints was evaluated to ascertain the enhancement in their capacities associated with each strengthening scheme. It is worth to mention here that in reinforcing these joints, the recommendations and guidelines previously provided by researchers were followed to achieve a reasonable and practical design for the provided reinforcement.

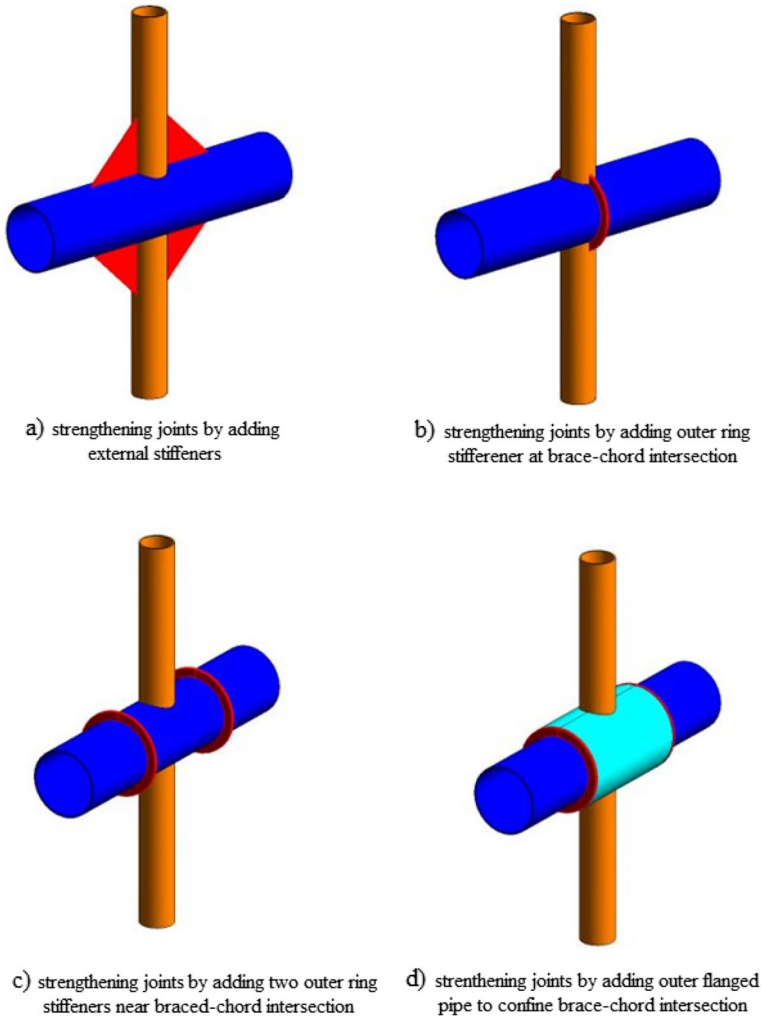

Fig. 1 Configuration of considered reinforced joints

Details of considered strengthening schemes

The first strengthening scheme is formed by connecting externally the brace to chord members by welding four triangular shape stiffeners at joint location as indicated in connection type (a) shown on Fig. 1. As can be noted, this scheme is applicable for both newly and already erected X-joints. It was initially proposed by [25] for strengthening CHS T-joints, then extended later for strengthening CHS X-joints [13, 26]. Performed studies concluded that this scheme could enhance the ultimate compressive strength and initial stiffness of CHS X-joints compared to those of unreinforced joints having the same dimensions by 27.2% and 13.3%, respectively. Also, it was noted that as unreinforced joints, reinforced joints experienced the same failure mode which is cord plastification. However, comparing with unreinforced joints, the reinforced joints experienced smaller deformation at brace and chord intersection. In addition, it was noted that the ratio of brace to chord diameter (β) and the ratio between stiffener length and brace chord diameter (η) have a significant effect on the level of enhancement for joints capacities. Joints with small β ratios showed better capacities enhancement compared to

joints with large β ratios. Also, it was found that variation to thickness of stiffeners has no effect on joints capacities.

The second considered scheme was that proposed by Zhu et al. [27, 28] and Yang et al. [24] in which a single ring stiffener is welded to both brace and chord at location of chord-brace intersection as shown in joint (b) in Fig. 1. Studies indicated that external stiffening ring can significantly increase both the ultimate compressive capacity and the initial stiffness of CHS X-joints. For instance, for X-joints having brace to chord diameter ratio of 0.25 reinforced using this scheme, the ultimate joints load capacities and initial stiffnesses were increased by 86% and 121%, respectively. In addition, the studies showed that the failure mode is dependent on ring width and thickness. For small ring width and stiffening ring thickness, the failure mode was chord plastification, while with increasing the ring size (including ring width and thickness), the failure mode was local buckling that occurred at the connection part of brace and ring. Further increase in stiffening ring size resulted in brace failure.

Recently, Melek et al. [15] proposed a third scheme for enhancing CHS X-joints by adding symmetrically two distant outer ring stiffeners welded to the chord on each side of the brace outside the brace-chord welding zone as in connection type (c) shown on Fig. 1. A comprehensive numerical study was performed, to examine the impact of different geometric design aspects for the stiffeners such as their diameters, thicknesses and spacing on the efficiency of such strengthening technique. Compared to the two previously indicating strengthening schemes, this technique has the advantages of avoiding the execution of any weld within the zone of the connection between brace and chord members, since these rings are located away from the chord-brace junction. In addition, it involves the utilization of minimum radius to ring stiffeners that keeps the aesthetic appearance of the structure unchanged. This proposed strengthening technique resulted in enhancing the strengths and initial stiffnesses of the joints compared to those of unreinforced joints by about 195.4% and about 120%, respectively in certain cases. Also, the study showed that with small width and thickness for stiffening rings the failure mode was yielding of chord, however, with increasing stiffener rings diameters and thickness, the mode of failure became brace yielding.

The fourth considered scheme in this study, was proposed by Gerges et al. [6]. It involves the utilization of two outer hollow ring flanges welded to additional pipe as in connection type (d) shown in Fig. 1. This technique was initially developed for strengthening CHS T-joints [14] then extended to strengthen CHS X-joints. The conducted numerical studies for this scheme examined, in addition to evaluating the gain in joints strengths and stiffnesses, the influence of different design aspects such as hollow ring flanges diameter, the stiffening pipe thickness, and length of the pipe for different values of brace diameter-to-chord diameter ratios. This strengthening technique resulted in great enhancement to joints strength to the degree that the increase in joints strengths reached 289.7% compared to strength of unreinforced joints for certain cases. Also, it resulted in great enhancement to joints stiffnesses. However, the execution process for such scheme seems rather complicated, since it requires the addition of two outer half cylindrical flanges welded together, then welded to chord and brace members which is considered extensive welding works but again away from chord-brace welded junction. Again, with thin outer flanges the failure mode was yielding of chord, however,

with increasing the thickness of the outer cylindrical flanges the mode of failure became brace yielding.

Verification of finite element models

As previously mentioned, the verification for the finite element models was carried out by comparing the results of six specimens that were tested experimentally by Li et al. [13] and Zhu et al. [25] against the obtained results from finite element analyses. The six tested specimens consisted of two unreinforced specimens designated in this research as X1 and X2 and four reinforced specimens designated as X3, X4, X5, and X6. The modelled reinforced specimens were two reinforced by external stiffeners (X3 and X4) and another two specimens reinforced by single outer ring stiffener at the brace-chord intersection (X5 and X6).

Unfortunately, there were no experimental tests available for the other two strengthening schemes. The models were developed using the software ANSYS 17 [1]. Figure 2 shows the finite element idealization for the unreinforced joints, while Figs. 3 and 4 show the finite element idealization for reinforced joints with external stiffener and single outer-ring stiffener, respectively.

Due to the symmetry in geometry and loading conditions, only half of the overall joint was modelled to decrease computational effort. The four-node shell element with six-degrees of freedom at each node "shell 181" available in ANSYS 17 software library was utilized to simulate the braces and chords walls. The steel material was simulated using bilinear isotropic hardening elastic perfectly plastic relationship between stress and strain.

Material properties for chords, braces and stiffeners were taken similar to those utilized in the experiments and are listed in Table 1, where E_o: Young's modulus of the

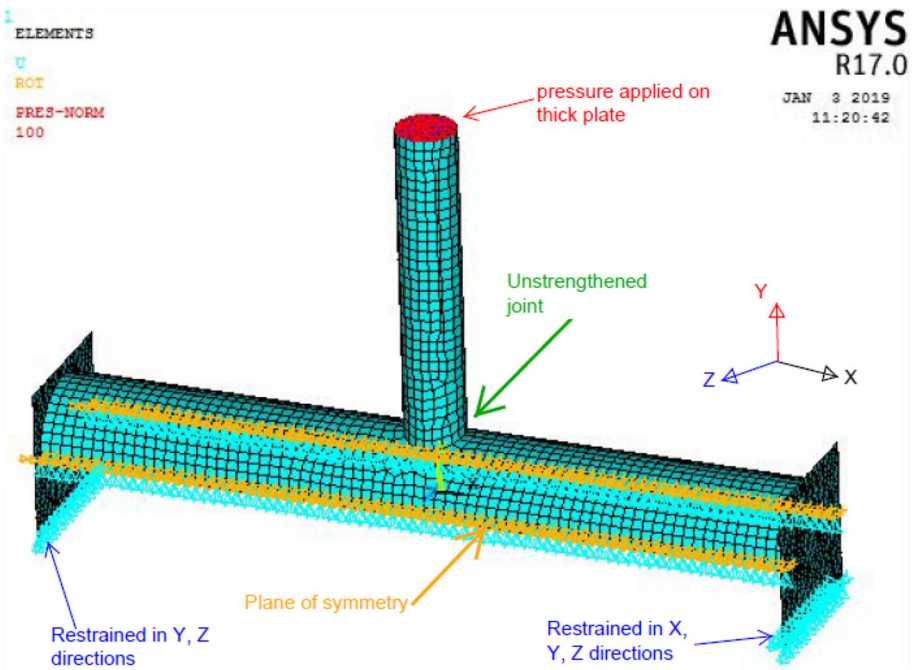

Fig. 2 Finite element idealization to unreinforced joint

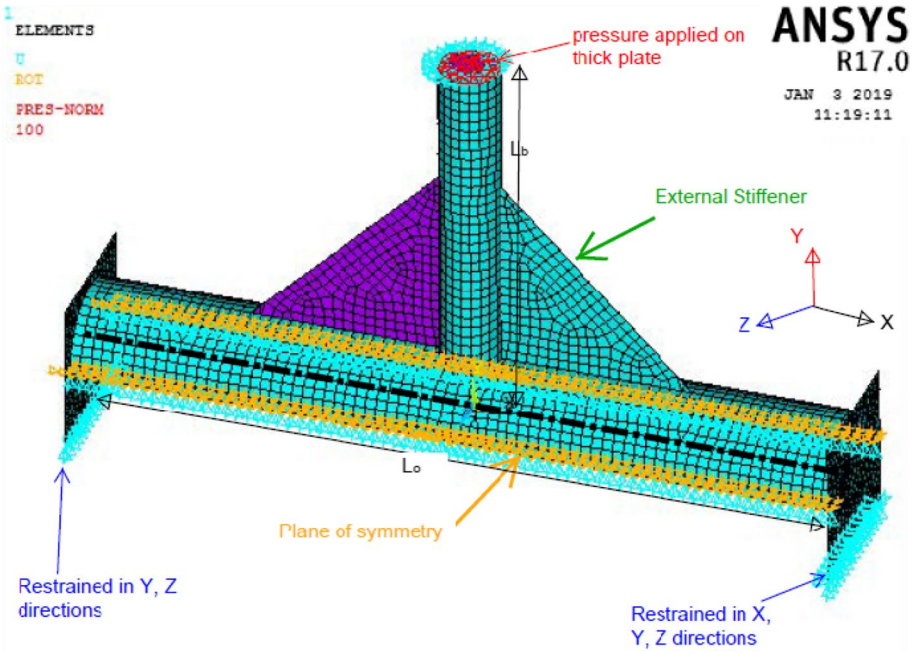

Fig. 3 Finite element idealization for joint reinforced by external stiffeners

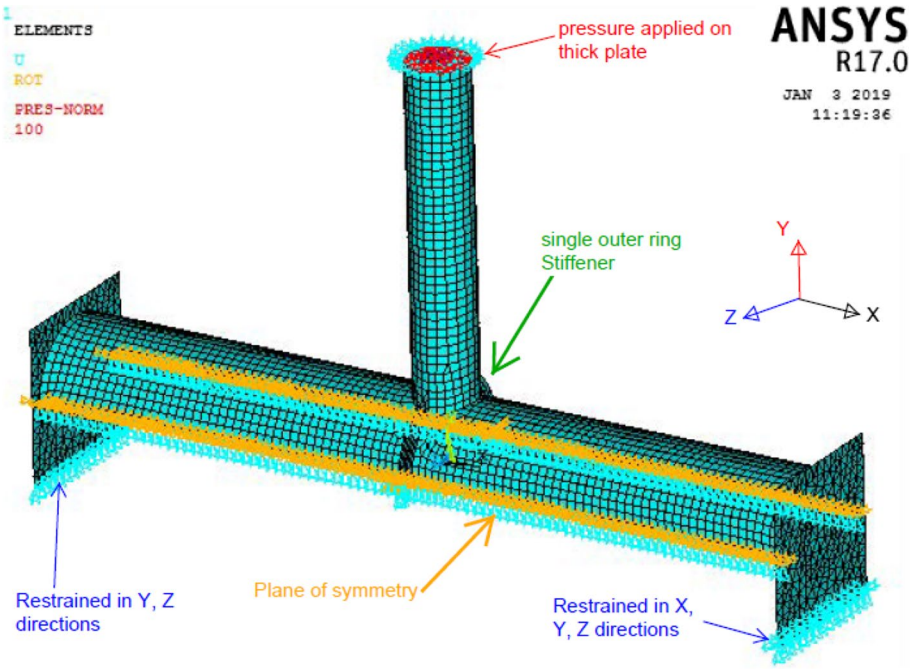

Fig. 4 Finite element idealization for joint reinforced by single outer ring stiffener

chord; E_b: Young's modulus of the brace, and E_a Young's modulus of the stiffeners, while f_{yo}: yield stress of the chord, f_{yb}: yield stress of the brace, and f_{ya}: yield stress of the stiffeners.

Table 1 Material properties for tested specimens by W. Li et al. and Zhu et al.

Reference	Specimen ID	E_o (GPa)	E_b (GPa)	E_a (GPa)	f_{yo} (MPa)	f_{yb} (MPa)	f_{ya} (MPa)
Li et al. [13]	X1	194	192	–	325	316	–
	X3	194	192	212	325	316	301
	X2	194	200	–	325	321	–
	X4	194	200	212	325	321	301
Zhu et al. [25]	X1	194	192	–	325	316	–
	X5	194	192	209	325	316	315
	X2	194	200	–	325	321	–
	X6	194	200	209	325	321	315

Table 2 Geometrical dimensions of experimentally tested specimens

Ref	Spec. ID	d_o mm	t_o mm	L_o mm	d_b mm	t_b mm	L_b mm	L_S/H_S mm	d_s mm	t_s mm
Li et al. [13]	X1	299.80	8.03	1806.4	151.73	8.11	752.60	–	–	–
	X3	299.60	8.02	1806.3	151.81	8.10	752.40	303.5	–	7.8
	X2	300.10	8.05	1801.4	218.40	8.05	1124.6	–	–	–
	X4	300.40	8.01	1796.9	218.00	8.03	1124.9	437.3	–	7.9
Zhu et al. [25]	X1	299.80	8.03	1806.4	151.73	8.11	752.60	–	–	–
	X5	299.60	8.05	1807.1	151.81	8.15	748.20	–	400	8.04
	X2	300.10	8.05	1801.4	218.43	8.05	1124.6	–	–	–
	X6	299.80	8.05	1806.1	218.03	8.02	1142.9	–	400	8.01

Geometrical dimensions of the tested specimens are listed in Table 2, where d_o is chord member diameter, t_o is chord member wall thickness, L_o is chord member length, d_b is brace member diameter, t_b is brace member wall thickness, L_b is brace member length, t_a is stiffener thickness, L_s/H_s is triangular stiffener width/height, d_s is ring stiffener outer diameter, and t_s is ring or triangular stiffener thickness. The weld between brace and chord members was assumed to be complete joint penetration following the mechanical properties of the chord, while its thickness was following the thickness of connected steel elements.

The brace axial load in the model was simulated by applying pressure on thick plate placed at brace tip to resembling the brace end plate utilized in the experiment and to ensure the uniformity of the load distribution. Two thick vertical plates were modeled and connected to chord's two ends. One of them was restrained both vertically in Y direction and laterally in Z direction and unrestrained longitudinally in X direction while the other was fully restrained translationally in the three directions. These plates were thick enough to avoid the occurrence of local failures at the location of supports of the chord. Fine meshing was provided around the joint region to obtain accurate results, while coarse meshing (elements with 25×25 mm) was applied at locations further from the joint region.

The results of the finite element models compared to the experimental outcomes for the considered specimens are represented in Figs. 5, 6, and 7 in the form of relationships between applied loads versus ovalization. The ovalization in this study was measured as the top vertical displacement of the brace member under axial load less its shortening.

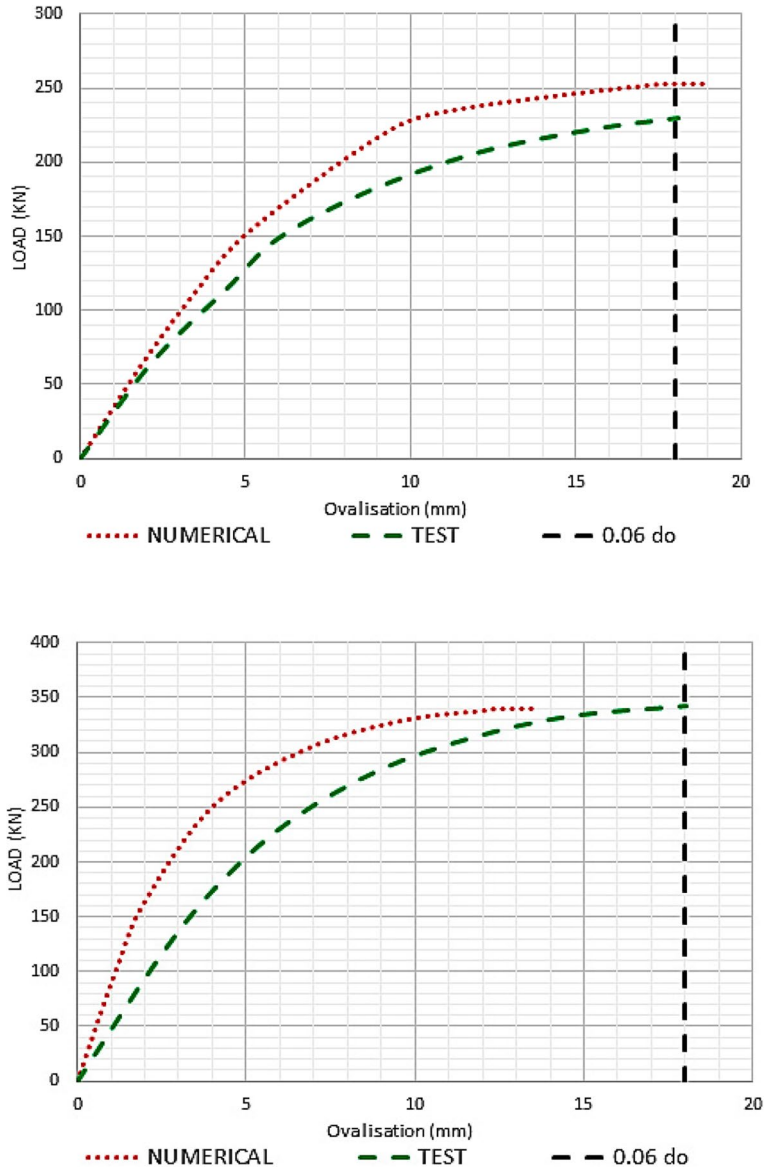

Fig. 5 Experimental versus numerical load-ovalisation relationships for specimen X1 and X2

As can be noted, there are good correlation between the FEM and the experimental test results which indicates the ability of the finite element models to represent the experimental behavior of the specimens with high degree of accuracy and reliability. It is worth to indicate here that the load-ovalization curves are plotted either until the load reached the peak load (as the behavior of the joints beyond the peak load is not a part of the current study) or until the ovalization reached the limit of 0.06 as mentioned by [3, 4]. This deformation limit is plotted as dashed line in these figures. Furthermore, Table 3 lists the nominal strengths that are obtained from the FEM for the considered specimens against those obtained from the tests.

Regarding the stress patterns, Fig. 8 shows the stress pattern obtained by Li et al. [13] for testing specimen X3 and that obtained by Zhu et al. [25] from testing

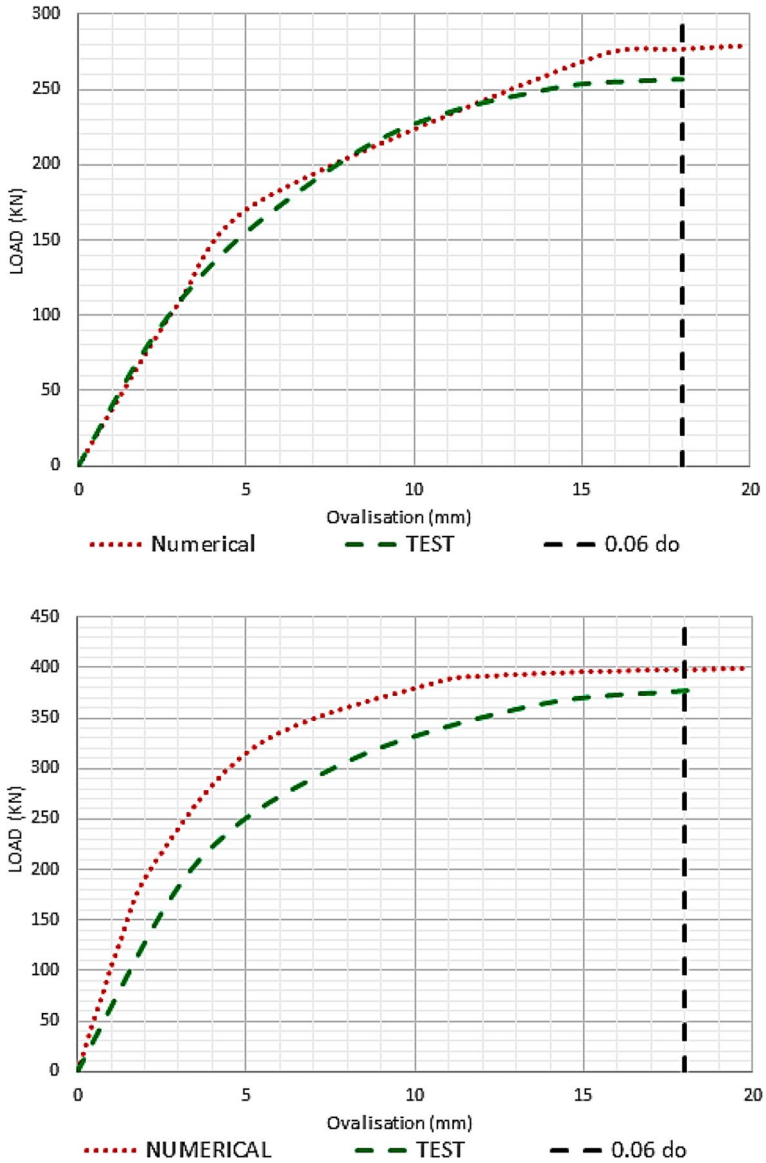

Fig. 6 Experimental versus numerical load-ovalization relationships for specimen X3 and X4

specimen X4 against the results obtained from finite element analyses. As can be noted, good correlation exists between test results and the developed finite element models in this study.

For the two additional reinforcing schemes that were not part of joints verification task, Figs. 9 and 10 show their finite element idealization.

Results and discussion

Geometry of studied joints

For this study, forty-five joints were developed and examined. They were divided into nine groups designated as A, B, C, D, E, F, G, H, and I. Each group contains five joints having the same chord/brace dimensions and mechanical properties as listed in Table 4.

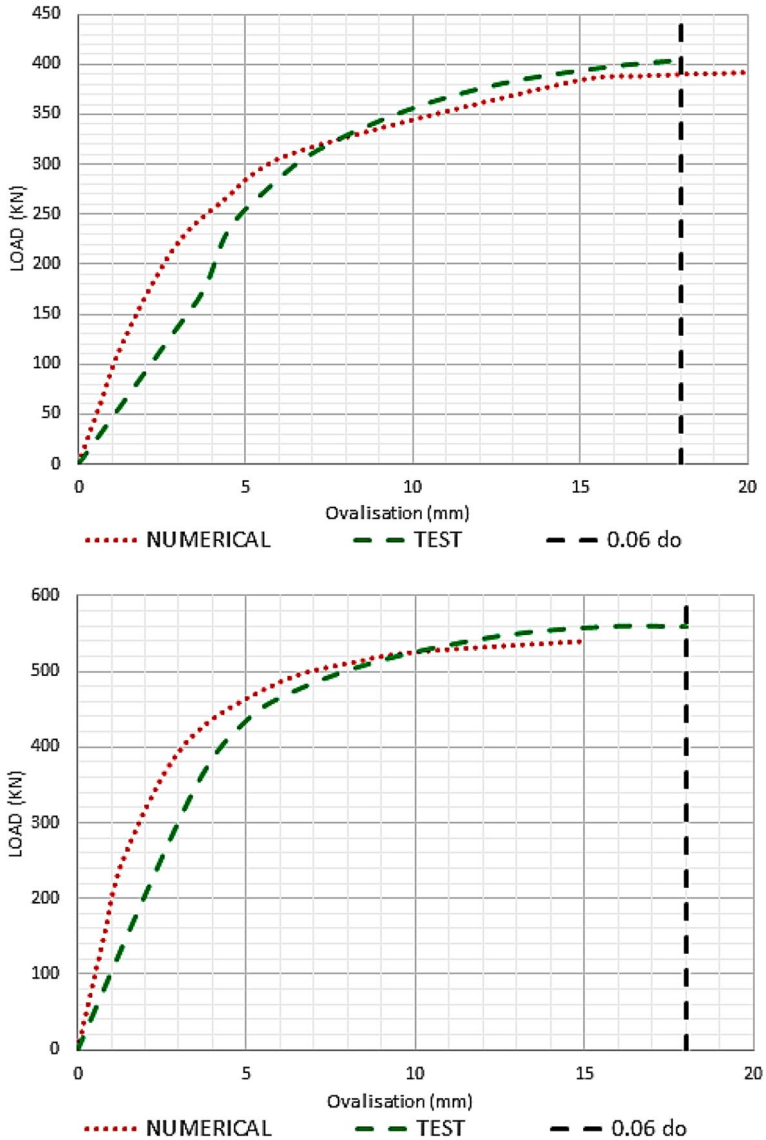

Fig. 7 Experimental versus numerical load-ovalisation relationships for specimen X5 and X6

Table 3 Comparison between the experimental and the numerical results

Reference	Spec. ID	Experimental nominal strength P_{test} (KN)	Numerical nominal strength P_{num}. (KN)	P_{test}/P_{num}	Error %
W. Li et al	X1	232.61	247.4	0.94	6.3%
	X3	263.35	277	0.95	5.1%
	X2	352.04	337.1	1.04	4.2%
	X4	375.55	398	0.94	5.9%
Zhu et al	X1	232.61	247.4	0.94	6.3%
	X4	408.07	389.25	1.05	4.6%
	X2	352.04	337.1	1.04	4.2%
	X6	557.6	540.04	1.03	3.1%
Average error %					4.9%

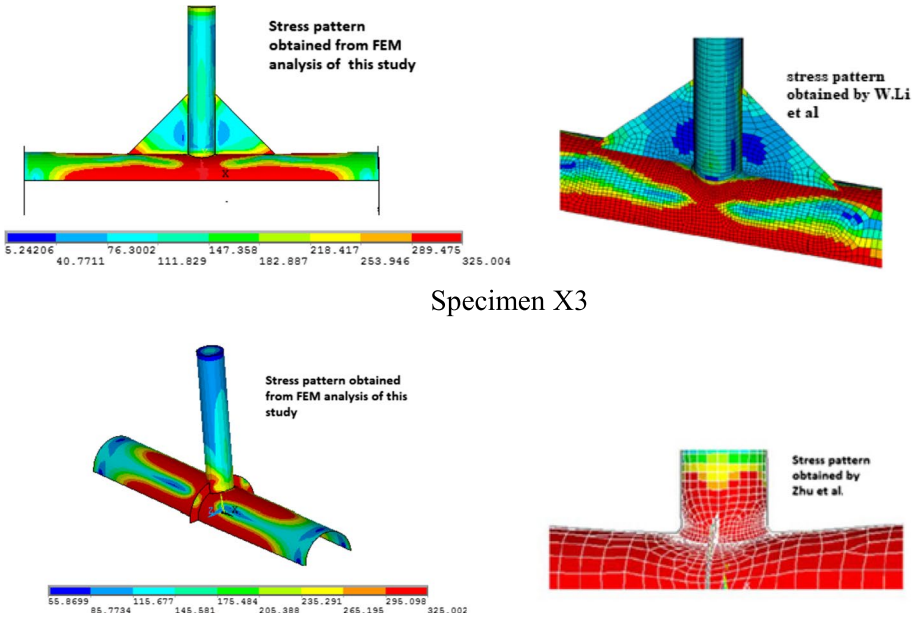

Fig. 8 Comparison between stress patterns obtained from FEM analysis and tests

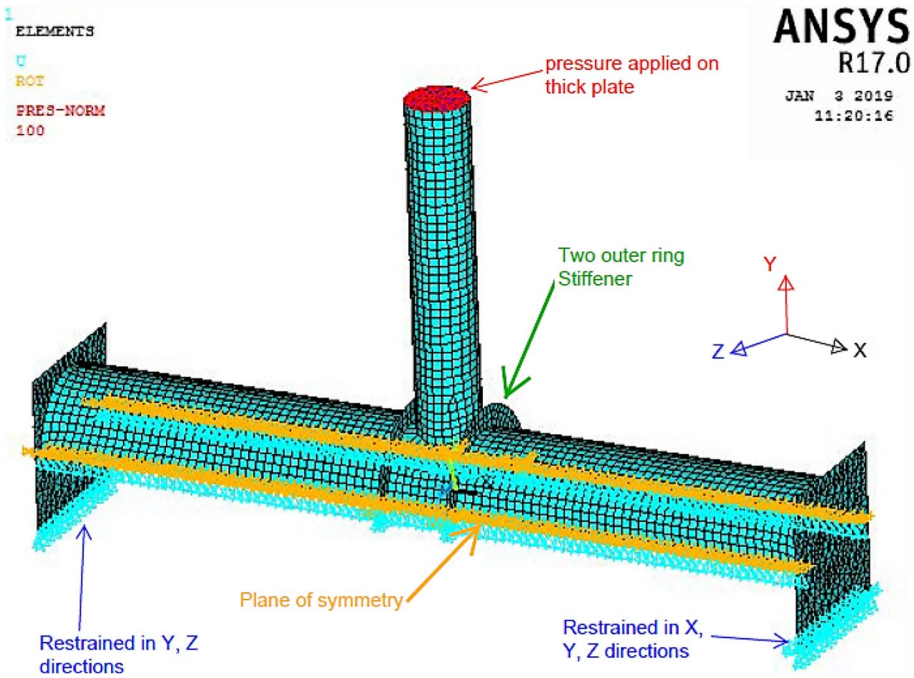

Fig. 9 Finite element idealization for joints reinforced by two outer ring stiffeners

One of the joints was unreinforced and employed as the base for comparison and the other joints each one of them was reinforced utilizing one the four considered strengthening schemes.

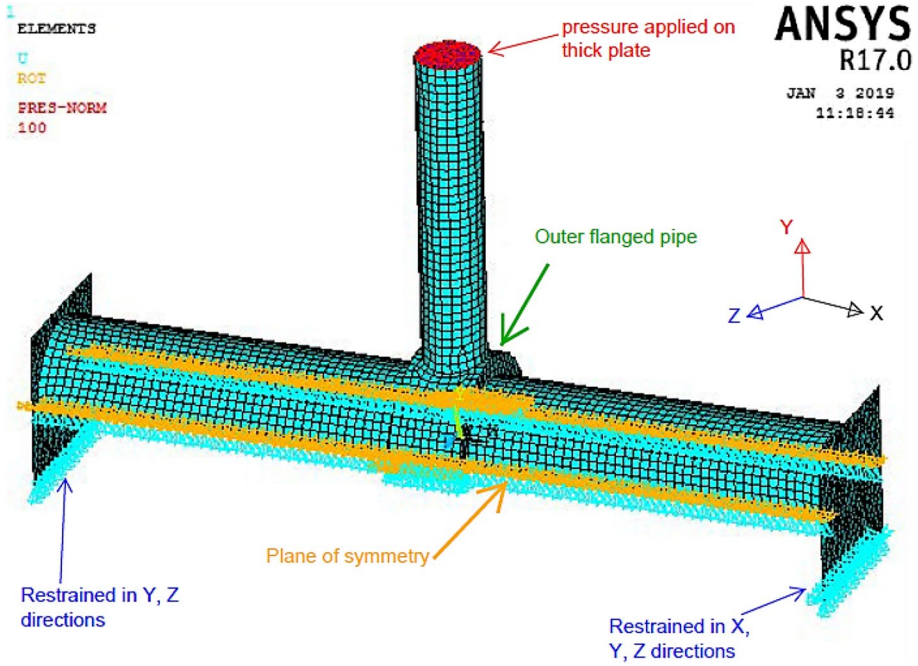

Fig. 10 Finite element idealization for joints reinforced by outer flanged pipe

Table 4 Geometrical dimensions and mechanical properties for the nine groups

Group	Chord Dim. (mm)		Brace Dim. (mm)		ɣ	β	E_o (GPa)	E_b (Gpa)	f_{yo} (Mpa)	f_{yb} (Mpa)
	d_o mm	t_o mm	d_b mm	t_b mm						
A	292	6	70	12	24.33	0.24	227	224	345	345
B	292	6	140	15	24.33	0.48	227	224	345	345
C	292	6	210	15	24.33	0.72	227	224	345	345
D	292	9	70	12	16.22	0.24	227	224	345	345
E	292	9	140	15	16.22	0.48	227	224	345	345
F	292	9	210	15	16.22	0.72	227	224	345	345
G	292	12	70	12	12.17	0.24	227	224	345	345
H	292	12	140	15	12.17	0.48	227	224	345	345
I	292	12	210	15	12.17	0.72	227	224	345	345

Close examination to Table 4 shows that the selected joints are covering wide range of CHS X-joints, since γ values are ranging from 12.2 to 24.3 and β values are ranging from 0.24 to 0.72, where γ is half the ratio between chord external diameter and its thickness and β is the ratio between the brace external diameter and chord external diameter. This selection for the specimens' dimensions allowed for evaluating the enhancement in the strengths and stiffnesses for the joints within each group due to employing different strengthening schemes. Moreover, having γ values unified for each three groups of joints allowed for conducting a comparison between the considered strengthening schemes including only the aspect of brace dimensions. Similarly unifying the β values for each three groups of joints allowed for conducting a

comparison between the considered strengthened joints including only the aspect of chord thickness. Regarding the utilized stiffeners, Table 5 lists the dimensions and design aspects for the added stiffeners to strengthen theses joints.

Study results

Figure 11 shows the axial load-ovalization relationship for each of the analyzed joint. In this figure, the relationships for the joints belonging to each group was plotted on the same graph to allow for visualizing the impact of adopting different reinforcing scheme on joints strengths and stiffnesses. In addition, a comparison was held between joints having the same γ values or having same β values to investigate the effects of brace

Table 5 Dimension of stiffening elements utilized for strengthening the studied joints

Group	Type	Stiffening elements dimensions (mm)		
A	External stiffener	$L_s = H_s = 225$		$t_s = 6$
	Single external ring	$d_s = 388$		$t_s = 12$
	Two external rings	$d_s = 388$	$l_s = 84$	$t_s = 6$
	External flanges pipe	$d_s = 388$	$l_s = 84$	$t_s = 4.5$
B	External stiffener	$L_s = H_s = 450$		$t_s = 6$
	Single external ring	$d_s = 388$		$t_s = 12$
	Two external rings	$d_s = 388$	$l_s = 84$	$t_s = 6$
	External flanges pipe	$d_s = 388$	$l_s = 84$	$t_s = 4.5$
C	External stiffener	$L_s = H_s = 660$		$t_s = 6$
	Single external ring	$d_s = 388$		$t_s = 12$
	Two external rings	$d_s = 388$	$l_s = 84$	$t_s = 6$
	External flanges pipe	$d_s = 388$	$l_s = 84$	$t_s = 4.5$
D	External stiffener	$L_s = H_s = 225$		$t_s = 9$
	Single external ring	$d_s = 388$		$t_s = 18$
	Two external rings	$d_s = 388$	$l_s = 84$	$t_s = 9$
	External flanges pipe	$d_s = 388$	$l_s = 84$	$t_s = 6.75$
E	External stiffener	$L_s = H_s = 450$		$t_s = 9$
	Single external ring	$d_s = 388$		$t_s = 18$
	Two external rings	$d_s = 388$	$l_s = 84$	$t_s = 9$
	External flanges pipe	$d_s = 388$	$l_s = 84$	$t_s = 6.75$
F	External stiffener	$L_s = H_s = 660$		$t_s = 9$
	Single external ring	$d_s = 388$		$t_s = 18$
	Two external rings	$d_s = 388$	$l_s = 84$	$t_s = 9$
	External flanges pipe	$d_s = 388$	$l_s = 84$	$t_s = 6.75$
G	External stiffener	$L_s = H_s = 225$		$t_s = 12$
	Single external ring	$d_s = 388$		$t_s = 24$
	Two external rings	$d_s = 388$	$l_s = 84$	$t_s = 12$
	External flanges pipe	$d_s = 388$	$l_s = 84$	$t_s = 9$
H	External stiffener	$L_s = H_s = 450$		$t_s = 12$
	Single external ring	$d_s = 388$		$t_s = 24$
	Two external rings	$d_s = 388$	$l_s = 84$	$t_s = 12$
	External flanges pipe	$d_s = 388$	$l_s = 84$	$t_s = 9$
I	External stiffener	$L_s = H_s = 660$		$t_s = 12$
	Single external ring	$d_s = 388$		$t_s = 24$
	Two external rings	$d_s = 388$	$l_s = 242$	$t_s = 12$
	External flanges pipe	$d_s = 388$	$l_s = 242$	$t_s = 9$

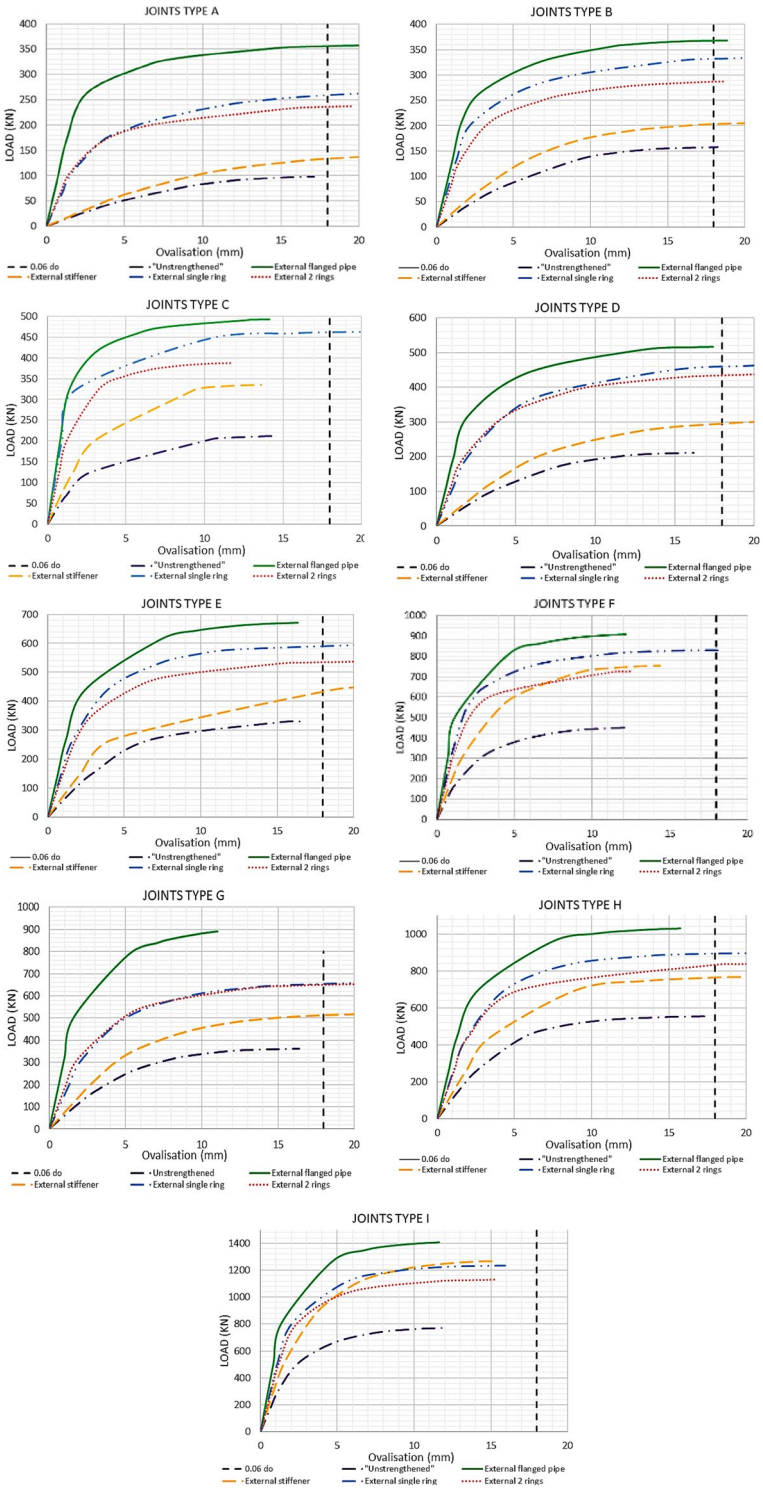

Fig. 11 Axial load-ovalization relationships for groups A, B, C, D, E, F, G, H, and I joints

dimensions, chord thickness and stiffeners design aspects on the behavior of reinforced joints. The following sections discuss in detail the findings of such comparisons.

Enhancement of joints axial strengths and stiffnesses

From examining the axial load-ovalization relationships, the joints maximum axial capacities can be determined. Figure 12 shows the axial compressive capacities for each of the analyzed joints. It is worth to indicate here, that the joints axial compressive strengths were determined as the load when joint reached weather the ovalization limit (0.06 d_o), yielding of the brace member or severe damage to the chord whichever is less. As can be noted, within each group, joints strengthened using external stiffeners achieved the minimum increase in joints strengths, while joints strengthened using external flange pipe achieved the maximum increase in joints strengths. Using single ring stiffener at brace-chord intersection or two external ring stiffeners resulted in intermediate increase in joints strengths with the former scheme giving higher increase in joints strengths compared to the later scheme. Regarding joints initial stiffnesses similar behavior was noted as shown in Fig. 13. Joints strengthened using external stiffeners achieved the minimum increase in joints stiffnesses, while joints strengthened using external flange pipe achieved the maximum increase in joints stiffnesses. Using single ring stiffener at brace-chord intersection or two external ring stiffeners resulted in intermediate increase in joints stiffnesses with the former scheme giving higher increase in joints stiffnesses compared to the later scheme.

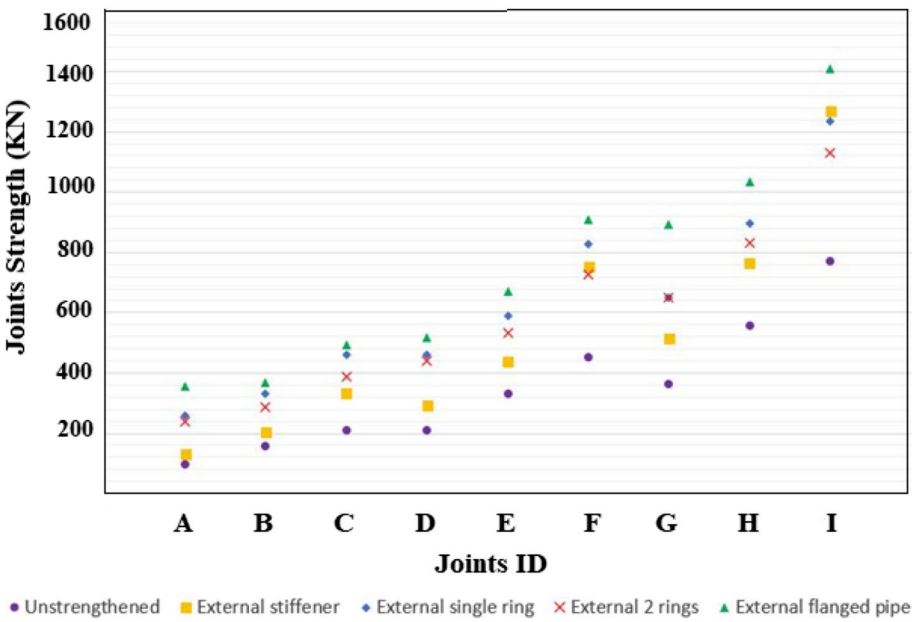

Fig. 12 Axial strength for the tested joints

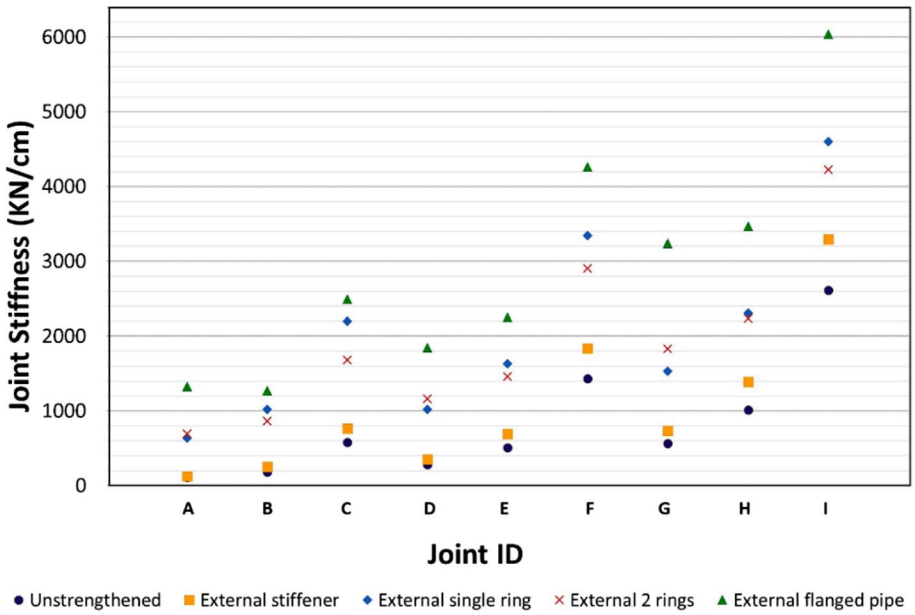

Fig. 13 Axial stiffness for the tested joints

Effect of β ratio on joints performance

By calculating the percentage of gain in strength for the joints using the following formula:

$$Percentage\ enhancment\ \% = \frac{strength\ of\ stiffened\ joint - strenght\ of\ unreinforced\ joint}{strenght\ of\ unreinforced\ joint} \times 100 \quad (1)$$

and plotting them against the β values as shown in Fig. 14 the following can be noted:

a. For joints having low, medium and high chord slenderness ratio (γ), the gains in joints strengths percentages due to stiffening them using external single ring, external two rings or external flanged pipe is reduced with increase in β value until it reaches a value of about 0.48, then the gain percentage in strength slightly increase after that. In other words, those schemes are more effective in strengthening joints having brace diameter relatively small compared to chord diameter. This is attributed to the fact that these schemes enhance joints strengths through reinforcing the chord walls at chord/brace joint locations which delays chord walls buckling or punching. However, when brace diameter became relatively large, a large portion of the axial forces can be transmit directly to chord sides reducing the demand on the chord top surface.

b. For joints having low, medium, and high chord slenderness ratio (γ), the gain percentage in strength achieved by utilizing external stiffener for strengthening CHS X-joints, is not affected much when the value of (β) is between 0.28 and 0.48 and remain constant. However, for joints where (β) is more than 0.48, the

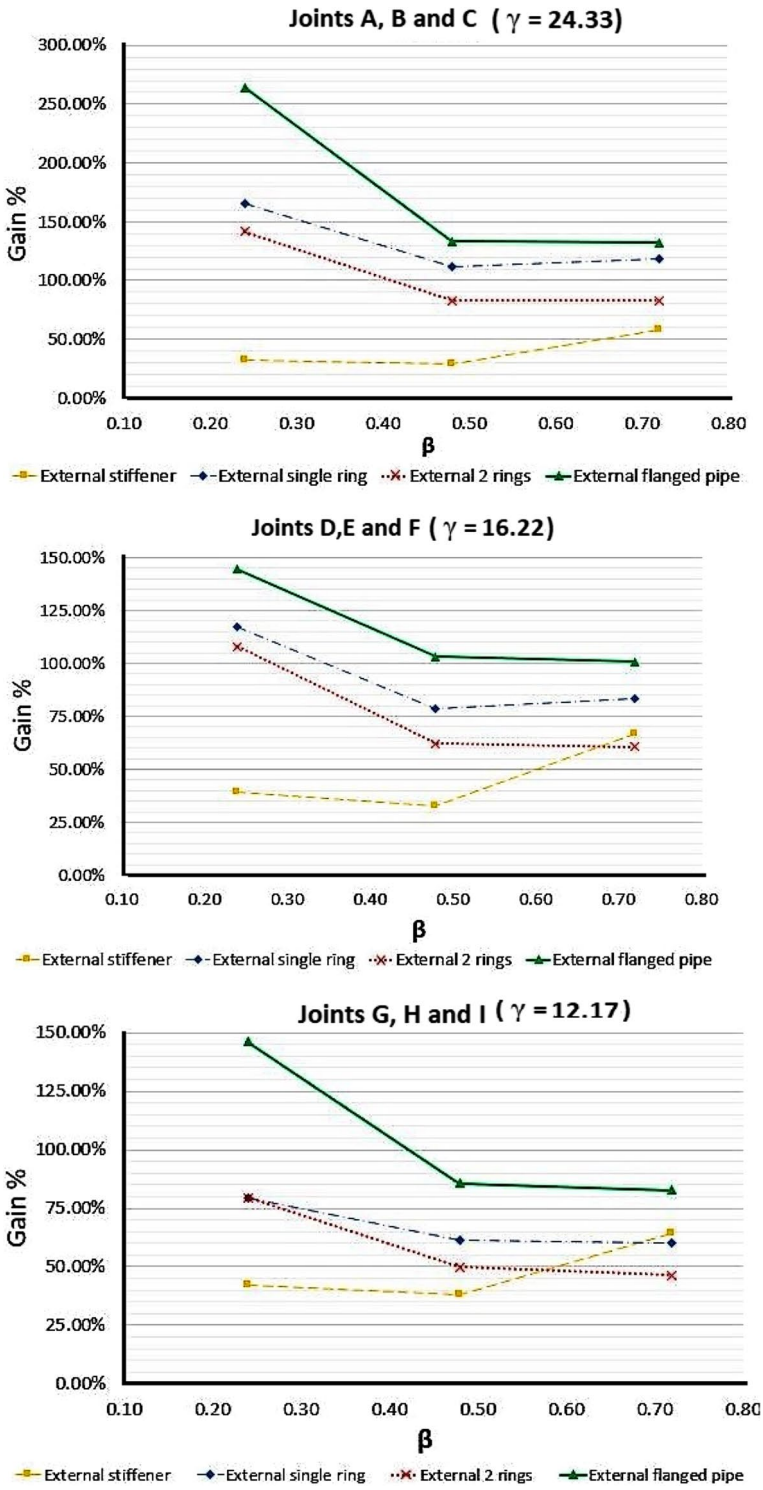

Fig. 14 Effect of β ratio on joints capacities enhancement for same γ ratio

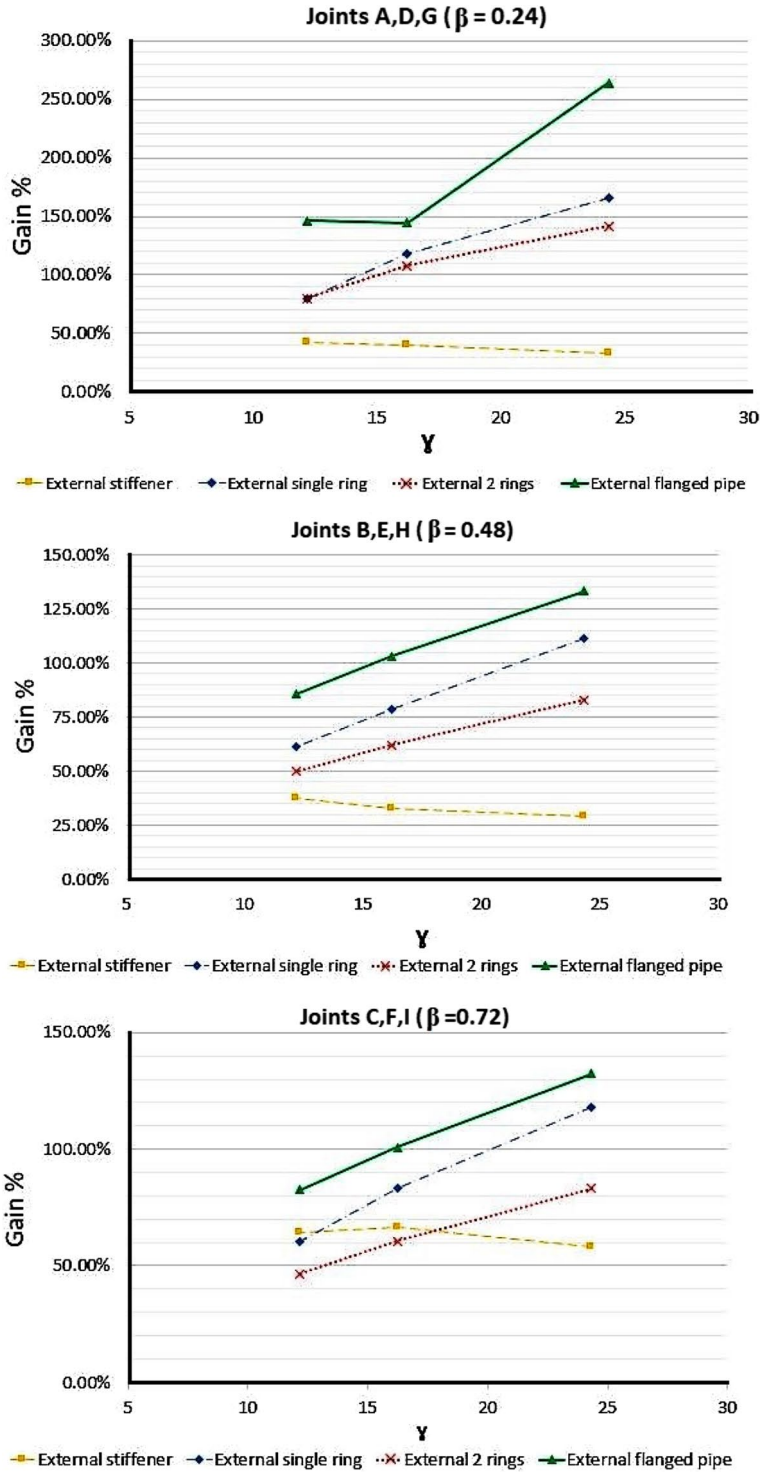

Fig. 15 Effect γ of ratio on joints capacities enhancement for same β ratio

gain percentage in joints strength increases as the (β) increases. This is attributed to the fact that gaining strength for joints utilizing this scheme is mainly due to the increase of the area of chord wall that engage in resisting the deformation which is relatively high with braces having diameters close to chord diameters.

Effect of γ ratio on joints performance

For joints having the same β ratios, like joints A, D, G and similarly, B, E, H and C, F, I the load-ovalization relationships were investigated and the relationships between the strength gain percentage for joints and γ ratios were plotted in Fig. 15. Examining this figure indicates that:

a) Utilizing external flanged pipe scheme for reinforcing CHS X-joints resulted in achieving the highest gain in joints strengths, while employing external stiffener scheme results in the lowest gain in joints strengths. Using external single ring stiffener or external two rings' stiffeners schemes for reinforcing CHS X-joints resulted in comparable intermediate gain to joints enhancement.
b) External flanged pipe, external single ring stiffener, and external two rings' stiffeners schemes are more effective when γ ratio has a high value.
c) The gains in joints strength when external stiffener strengthening scheme utilized did not dependent on chord thickness, rather they are affected by the brace's diameters.

To get more deeper insight to this phenomenon, a further investigation to the performance of strengthened joints with emphasis on the effects of the geometric dimensions and geometrical configurations of the utilized strengthening stiffeners was conducted. In this regard, the dimensions of the utilized stiffeners for each strengthening scheme were changed to force the failure criteria of the joint to be yielding of brace member rather than damage of the joint.

The study was carried out following the same finite element modeling, loading, and boundary conditions indicated before. Several iterations were performed to determine the geometrical dimensions of the stiffening elements that prevent local failure of the joints and limiting the failure to the state of yielding of the brace members which designated in this study as global failure to allow for full utilization of the members. The study was conducted through comparing the performance of three groups of joints designated as A1, A2, and A3 and their geometrical and mechanical properties are listed in Table 6.

Table 6 Geometrical parameters and mechanical properties of analyzed specimens

Group	Chord Dim. (mm)		Brace Dim. (mm)		ɣ	β	E_0 (MPa)	E_b (MPa)	f_{y0} (MPa)	f_{yb} (MPa)
	d_o	t_o	d_b	t_b						
A1	292	6	70	6	24.33	0.24	227	345	224	240
A2	292	9	140	6	16.22	0.48	227	345	224	240
A3	292	12	210	6	12.17	0.72	227	345	224	240

Table 7 Stiffening elements dimensions, joints capacities, and governing mode of failure for each joint

Joint ID	Type	Stiffening elements dimensions (cm)			Joint capacity KN	Governing failure mode
First iteration						
A1	External stiffener	$L_s = H_s = 225$		$t_s = 6$	142	Local failure
	Single external ring	$d_s = 388$		$t_s = 6$	183	Local failure
	Two external rings	$d_s = 388$	$l_s = 84$	$t_s = 6$	223	Local failure
	External flanged pipe	$d_s = 388$	$l_s = 84$	$t_s = 6$	313	Global failure
A2	External stiffener	$L_s = H_s = 450$		$t_s = 9$	414	Local failure
	Single external ring	$d_s = 388$		$t_s = 9$	416	Local failure
	Two external rings	$d_s = 388$	$l_s = 84$	$t_s = 9$	510	Local failure
	External flanges pipe	$d_s = 388$	$l_s = 84$	$t_s = 9$	626	Global failure
A3	External stiffener	$L_s = H_s = 660$		$t_s = 12$	852	Local failure
	Single external ring	$d_s = 388$		$t_s = 12$	845	Local failure
	Two external rings	$d_s = 388$	$l_s = 242$	$t_s = 12$	957	Global failure
	External flanges pipe	$d_s = 388$	$l_s = 242$	$t_s = 12$	957	Global failure
Second iteration						
A1	External stiffener	$L_s = H_s = 225$		$t_s = 10.8$	143	Local failure
	Single external ring	$d_s = 484$		$t_s = 6$	262	Local failure
	Two external rings	$d_s = 484$	$l_s = 84$	$t_s = 6$	311	Global failure
A2	External stiffener	$L_s = H_s = 450$		$t_s = 16.2$	414	Local failure
	Single external ring	$d_s = 484$		$t_s = 9$	538	Local failure
	Two external rings	$d_s = 484$	$l_s = 84$	$t_s = 9$	630	Global failure
A3	External stiffener	$L_s = H_s = 660$		$t_s = 21.6$	852	Local failure
	Single external ring	$d_s = 484$		$t_s = 12$	935	Global failure
Third iteration						
A1	Single external ring	$d_s = 584$		$t_s = 6$	313	Global failure
A2	Single external ring	$d_s = 584$		$t_s = 9$	632	Global failure

Table 7 shows the geometrical dimensions of the stiffeners that were chosen for strengthening each joint for the different trials. As can be observed, in the first trial, the assumed dimensions for the stiffeners were selected according to the recommendation of the strengthening schemes developers. The reinforced specimens were subjected to axial compressive forces and joint axial capacity and associated mode of failure were recorded. If the mode of failure was local joint failure (excessive deformation or yielding to chord at joint location with brace) the stiffening elements dimensions were increased, and new analyses were performed. The process continues until the mode of failure became global failure (yielding of brace) or we reached the maximum limits for dimensions provided by the strengthening scheme developers. The results of these analyses are listed in Table 7.

For external stiffener scheme, the external stiffeners dimensions (lengths and heights) were chosen to be equal to three times the brace diameter as these are the most effective dimensions recommended based on Li et al. work [13]. For the thickness of the external stiffener, the first iterations started with λ equal to 1, where λ is defined as the stiffener thickness parameter (t_s/t_o, ratio of stiffener thickness to chord thickness), then in the second iteration the stiffener thickness parameter increased to 1.8 which is the maximum limit utilized by Li et al. [13] in their research. In both iterations the joints failures

were local failures. Also, increasing the thickness of the stiffeners did not increase the joints capacities as indicated in Table 7. This conclusion is with line with the conclusion given in Li et al. studies [13]. Consequently, for this scheme, strengthening will increase joints capacities; however, local failure mode will be the most probably failure mode governing the behavior of these reinforced joints regardless of increasing the stiffeners dimensions.

For external single ring scheme, diameter of the external ring stiffener was initially chosen to be equal to 1.33 the diameter of the chord as recommended by Zhu et al. [25] and the ring thickness factor was taken equal to 1.0, where the ring thickness factor is defined as the ratio between stiffening ring thickness and chord wall thickness. In the first iteration, the joints failures were local failures. Then, the external ring stiffeners diameters were gradually increased in subsequent iterations, while the ring stiffeners were kept equal to the chords wall thicknesses until specimens' failure became global. Therefore, to have a global failure for joints strengthening with this scheme the diameter of the ring needs to be double the chord diameter which may be aesthetically questionable.

For the external two rings scheme, the two rings' stiffeners diameters were chosen initially to have 1.33 the diameter of the chord and the rings thickness factors were selected equal to 1.0. Only specimen A3 in this iteration experienced global failure, while specimens A1 and A2 continued to fail locally. In subsequent iterations, with increasing the diameters of the two rings stiffeners, all specimens failed globally. Consequently, compared to previous strengthening scheme, the gain in joints capacities can be achieved with more aesthetically appealing appearance due to small diameters of utilized ring stiffeners and has even the advantage of welding the ring stiffeners away from brace-chord welding zone.

For the external flanged pipe scheme, the gain in joints capacities was superior when he external flanged pipe diameter was chosen to be equal to 1.33 that of the chord diameter and its thickness is same as that of the chord and the failure was global one. However, the only drawback with this strengthening scheme is the additional material required, the complicated fabrication procedure and the extensive welding required.

Conclusions

This study presents an evaluation to the performance of four different external strengthening schemes that are mostly utilized for enhancing the capacities of CHS X-joints. The examined strengthening schemes were adding external stiffeners, adding single outer ring stiffener at brace-chord intersection, adding two outer ring stiffeners near brace-chord intersection, and adding outer flanged pipe to confine brace-chord intersection. The enhancement for joints' capacities were assessed in terms of the gain in joints axial compressive strengths and the improvement in joints stiffnesses. Within this study, 67 joints were analyzed as part of both the primary and auxiliary studies. The study concluded that

1. Among the studied strengthening schemes for joints, utilization of outer flanged pipe scheme resulted in the maximum gain to joints capacities (strength and stiff-

ness). With proper dimension adopting this scheme can shift damage to brace member resulting in full utilization of the members. However, the only drawback associated with the utilization of this strengthening scheme is the complicated fabrication process which involves manufacturing many steel parts (two hollow half circular pipes each equipped with two half outer hollow ring flanges), then welding these parts together and to the original joint.

2. Although utilizing external stiffeners for strengthening joints enjoys easiness from fabrication point of view, the gain in joints capacities associated with the implementation of this scheme is minimum. Even with the use of large and thick unacceptable aesthetically stiffeners, the joint remained the weakest point in the sub-assemblage.

3. When an external single ring stiffener or two ring stiffeners strengthening schemes were employed, the achieved gains in reinforced joints capacities were sufficient and with adopting rational diameters and thicknesses for the ring stiffeners in both cases, the modes of joints failure can be global modes indicating full utilization of the members in addition to ease of fabrication. However, it is worth to note here that using two ring stiffeners scheme compared to single ring stiffener scheme in reinforcing joints has the advantage of being more aesthetically appealing due to employing small diameter for ring stiffeners, in addition, to welding these stiffeners away from the location of brace intersection with chord which can have the benefit of reducing the residual stresses within the joint.

4. The study showed that the gain in joints strengths due to stiffening them using external single ring, external two rings or external flanged pipe is reduced with increase in β value until it reaches a value of about 0.48, then the gain percentage in strength is slightly increased after that. This attributed to the fact that brace diameter became large enough to transmit its axial forces directly to the chord pipe sides and avoid loading the chord pipe top surface. Also, it showed that utilizing external stiffener for strengthening CHS X-joints, is not affected much when the value of (β) is between 0.28 and 0.48 as gain in strengths remain constant. However, for joints where (β) is more than 0.48, the gain percentage in joints strengths increases as the (β) increases.

5. This study provided a methodology that can be followed in future to compare between the efficiency of different strengthening schemes for CHS X-joints other than those addressed in this research.

Abbreviations

CHS	Circular hollow section
β	Brace diameter-to-chord diameter ratio
γ	Chord diameter-to-chord thickness ratio
λ	Stiffener thickness parameter
η	Ratio between stiffener length and brace chord diameter
d_o	Chord member diameter
t_o	Chord member wall thickness
L_o	Chord member length
d_b	Brace member diameter
t_b	Brace member wall thickness
L_b	Brace member length
L_s	Triangular stiffener width
H_s	Triangular stiffener height

d_s	Ring stiffener outer diameter
t_s	Ring or triangular stiffener thickness.
l_s	Distance between ring stiffeners or length of flanged pipe
E_o	Young's modulus of the chord
E_b	Young's modulus of the brace
E_a	Young's modulus of the stiffeners
f_{yo}	Yield stress of the chord
f_{yb}	Yield stress of the brace
f_{ya}	Yield stress of the stiffeners
P_{test}	Experimental nominal strength
P_{num}	Numerical nominal strength

Acknowledgements
Not applicable

Authors' contributions
AO interpreted the results and draw the graphs and wrote the paper. PG performed the finite element analysis and achieved the results. SG edited the manuscript. All authors read and approved the final manuscript.

Funding
Not applicable.

Availability of data and materials
All data generated or analyzed during this study are included in this published article.

Declarations

Competing interests
The authors declare that they have no competing interests.

Received: 26 February 2023 Accepted: 1 May 2023
Published online: 09 May 2023

References

1. ANSYS program. Release 17 user's manual (2016). Swanson analysis system
2. Choo. Y.S. (1994), Strength evaluation of X-joints internally stiffened with longitudinal diaphragms, Proceedings of the International Offshore and Polar Engineering Conference, Osaka, Japan, April,21–29.
3. Choo YS, Van der Vegte GJ, Zettlemoyer N, Li BH, Liew JYR (2005) Static strength of T-joints reinforced with doubler or collar plates. I: experimental investigations. J Structural Eng 131(1):119–128. https://doi.org/10.1061/(ASCE)0733-9445(2005)131:1(119)
4. Choo YS, Zettlemoyer N, Li BH, Liew JYR (2005) Static strength of T-joints reinforced with doubler or collar plates. II: numerical simulations. J Structural Eng 131(1):129–138. https://doi.org/10.1061/(ASCE)0733-9445(2005)131:1(129)
5. Feng R, Young B (2009) Behavior of concrete-filled stainless-steel tubular X-joints subjected to compression. Thin Walled Struct 47(4):365–374. https://doi.org/10.1016/j.tws.2008.09.006
6. Gerges P, Gaawan S, Osman A (2020) Axial strength of steel CHS X-joints strengthened by flanged larger pipe. Can J Civ Eng 47(3):301–316. https://doi.org/10.1139/cjce-2018-0804
7. Guo Z, Li C, Zhu Q , Chen Y (2021), Behavior of partially concrete-filled X-joints with CHS braces and SHS chord under axial compression. J Constr Steel Res, 184.
8. Lan X, Wang F, Ning C, Xu X, Pan X, Luo Z (2016) Strength of internally ring stiffened tubular DT- joints subjected to brace axial loading. J Constr Steel Res 125:88–94. https://doi.org/10.1016/j.jcsr.2016.06.012
9. Lee MMK, Llewelyn-Parry A (2004) Offshore tubular T-joints reinforced with internal plain annular ring stiffeners. J Struct Eng 130(6):942–951. https://doi.org/10.1061/(ASCE)0733-9445(2004)130:6(942)
10. Lee MMK, Llewelyn-Parry A (2005) Strength prediction for ring-stiffened DT-joints in offshore jacket structures. Eng Struct 27(3):421–430. https://doi.org/10.1016/j.engstruct.2004.11.004
11. Lesani M, Bahaari MR, Shokrieh MM (2013) Numerical investigation of FRP strengthened tubular T-joints under axial compressive loads. Compos Struct 100:71–78. https://doi.org/10.1016/j.compstruct.2012.12.020
12. Lesani M, Bahaari MR, Shokrieh MM (2014) Experimental investigation of FRP strengthened tubular T-joints under axial compressive loads. Constr Build Mater 53:243–252. https://doi.org/10.1016/j.conbuildmat.2013.11.097
13. Li W, Zhang S, Huo W, Bai Y, Zhu L (2018) Axial compression capacity of steel CHS X-joints strengthened with external stiffeners. J Constr Steel Res 141:156–166. https://doi.org/10.1016/j.jcsr.2017.11.009
14. Melek PG, Hussein M, Gaawan S (2017) Confining T-joints by adding two outer hollow ring flanges welded to additional hollow circular pipe. Can J Civ Eng 44:783–801. https://doi.org/10.1139/cjce-2017-0065
15. Melek PG, Gaawan S, Osman A (2020) Strengthening steel CHS X-joints subject to compression by outer ring stiffeners. Int J Steel Structures 20(4):1115–1134. https://doi.org/10.1007/s13296-020-00346-0
16. Nassiraei H, Lotfollahi-Yaghin MA, Ahmadi H (2016) Static strength of collar plate reinforced tubular T/Y-joints under brace compressive loading. J Constr Steel Res 119:39–49. https://doi.org/10.1016/j.jcsr.2015.12.011
17. Nassiraei H, Lotfollahi-Yaghin MA, Ahmadi H (2016) Structural behavior of tubular T/Y-joints with collar plate under static in-plane bending. J Constr Steel Res 123:121–134. https://doi.org/10.1016/j.jcsr.2016.04.029

18. Nassiraei H, Lotfollahi-Yaghin MA, Ahmadi H (2016) Static strength of offshore tubular T/Y-joints reinforced with collar plate subjected to tensile brace loading. Thin-Walled Struct 103:141–156. https://doi.org/10.1016/j.tws.2016.02.010
19. Nassiraei H, Lotfallahi MA, Ahmadi H, Zhu L (2017) Static strength of doubler plate reinforced tubular T/Y- joints under in-plan bending load. J Constr Steel Res 136:49–64. https://doi.org/10.1016/j.jcsr.2017.05.009
20. Nassiraei H, Zhu L, Lotfallahi MA, Ahmadi H (2017) Static capacity of tubular X-joints reinforced with collar plate subjected to brace compression Thin-walled. Structure 119:256–265. https://doi.org/10.1016/j.tws.2017.06.012
21. Nassiraei. H., and Rezadoost P. (2021), Static capacity of tubular X-joints reinforced with fiber reinforced polymer subjected to compressive load. Engineering structures. 263:112041. https://doi.org/10.1016/j.engstruct.2021.112041
22. Shao Y-B, Lie S-T, Chiew S-P (2010) Static strength of tubular T-joints with reinforced chord under axial compression. Adv Struct Eng 13(2):369–377. https://doi.org/10.1260/1369-4332.13.2.369
23. Van der Vegte, G.J., Lera, D.H. and Owo, Y.S. (1997), The axial strength of uniplanar X-joints reinforced by T-shaped ring-stiffeners, Proceedings of the seventh international offshore and polar engineering conference, Honolulu, Hawaii, USA, May.
24. Yang K, Zhu., L., Bai. Y., Sun. H. and Wang. M. (2018) Strength of external ring stiffened tubular X-joints subjected to brace axial compression loading. Thin-Walled Structures 133:17–26. https://doi.org/10.1016/j.tws.2018.09.030
25. Zhu L, Zhao Y, Li S, Huang Y, Ban L (2014) Numerical analysis of the axial strength of CHS T-joints reinforced with external stiffeners. Thin-Walled Structures 85:481–488. https://doi.org/10.1016/j.tws.2014.09.018
26. Zhu L, Song Q, Bai Y, We Y, Ma L (2017) Capacity of steel CHS T-joints strengthened with external stiffeners under axial compression. Thin-Walled Structures 113:39–46. https://doi.org/10.1016/j.tws.2017.01.007
27. Zhu L, Han S, Song Q, Ma L, Wei Y, Li S (2016) Experimental study of the axial compressive strength of CHS T-joints reinforced with external stiffening rings. Thin-Walled Structures 98:245–251. https://doi.org/10.1016/j.tws.2015.09.029
28. Zhu L, Yang K, Bai Y, Sun H, Wang M (2017) Capacity of steel CHS X-joints strengthened with external stiffening rings in compression. Thin-Walled Structures 115:110–118. https://doi.org/10.1016/j.tws.2017.02.013

Publisher's Note